JOURNAL OF APPLIED ELECTROCHEMISTRY 15 (1985) 251–257

Faradaic impedance measurements of small magnitudes encountered in high capacity electrical storage cells

S. A. G. R. KARUNATHILAKA, R. BARTON, M. HUGHES, N. A. HAMPSON

Department of Chemistry, University of Technology, Loughborough, Leics. LE11 3TU, UK

Received 6 February 1984; revised 29 June 1984

Gross errors in impedance measurements of high capacity electrical storage cells can be observed when using a commercial Frequency Response Analyser (FRA) coupled with an electrochemical interface. The magnitudes of these errors are discussed and an appropriate automatic calibration procedure is described which enables the correct impedance to be recorded at any frequency.

1. Introduction

During the measurement of cell impedance values typically less than 0.1 Ω, the impedance of the connecting leads is also significant. Even though the frequency independent ohmic resistance of the leads could be easily subtracted, the frequency dependent reactance of lead inductance and stray capacitance tend to distort the actual impedance spectrum of the test system. These errors could be minimized by the use of two separate leads for the current flow and another two for sensing the ac voltage. A further complication in the measurement of low impedances is the selection of a sense resistor of the same order of magnitude as the test system. Since the sense resistance should be of the order of 0.1 Ω its inductance also becomes significant as a 0.2 μH inductance at 10 kHz has a reactance of 0.015 Ω, which cannot be neglected when compared with a resistance of 0.1 Ω. The sense resistor should therefore be regarded as a 'sense impedance', having a non-zero imaginary part. When such a resistor is incorporated in an interfacing device for the measurement of the cell current, the effective impedance will be composed of the actual impedance of the resistor plus the impedance of the electronic components together with the leads through which the cell current flows within the interfacing device. Even though the latter contribution is negligible for normal sense resistance values, i.e. $> 10\,\Omega$, it is appreciable for low values ($\sim 0.1\,\Omega$ and less) of sense resistors. This impedance component will generally vary with frequency and the effective impedance of the sense resistance will be a complicated frequency dependent function which cannot be measured directly. This paper outlines the techniques developed for the estimation of the effective impedance of the sense resistor and the subsequent measurement of impedances of low magnitudes without the gross errors arising from the interference from the connecting lead.

2. Experimental details

The aim of the general investigation was the measurement of the faradaic impedance of the 23 Ah Ni–Cd and sealed lead–acid cells used in aircrafts and to study the variation of impedance and kinetic parameters of the cells with state-of-charge. The experimental set-up consisted of a Frequency Response Analyser (FRA) (Solartron 1250) coupled to an electrochemical interface (Solartron 1186) which was used to poise the cells at Open Circuit Voltage (OCV) and to perturb the potential with the external ac signal. The FRA was commanded by a computer (Kemitron 3000) which also processed the results.

The 1186 interface was operated in the 2-terminal mode with the secondary electrode and Reference 1 terminals shorted together to form the positive terminal, and the working electrode and Reference 2 terminals shorted together to form the negative terminal.

0021–891X/85 $03.00 + .12

2.1. *Cell connection*

The 1 m long coaxial cables supplied by Solartron for the connection of the cell were found to be unsuitable as they increased the cell resistance by 0.05 Ω and added an inductive reactance of 0.1 Ω at 50 kHz. The use of 'crocodile' clips and push fit plugs were also found to increase the cell impedance significantly. In order to avoid such connections it was decided to use two short lengths (~ 20 cm) of tinned copper wires of Standard Wire Gauge (SWG) 18, bolted at the centre to the cell terminals with the free ends connected to the respective terminals of the electrochemical interface. The measurements carried out with different thicknesses of copper wires connected in this way did not show any variation of the impedance with the thickness of the wire. However, quite unsuitable connections resulted if the centres of the wires were soldered to spade clips for connection to the cell terminals and the results showed an increase of about 10 mΩ in the cell resistance. This was due to the ohmic resistance of the soldered junction and the 'spade' clip. The use of a single wire in the absence of soldered joints had the advantage of providing two separate paths for the flow of dc current and for the superimposition of the ac signal; any additional resistance due to ohmic drop was thereby avoided. However, the impedance of the battery terminals cannot be isolated from the impedance of the actual faradaic impedance of the cell as both ac and dc currents flow through these terminals.

2.2. *Sense resistor*

Fig. 1 shows the impedance spectrum of a typical 25 Ah sealed lead–acid cell using the lowest sense resistor available with the commercial interface (10 Ω). An extensive inductive region is observed at high frequency which has been discussed in an earlier connection [1] but for which a satisfactory interpretation is lacking. It is now believed that although such inductive regions occur under certain kinetic circumstances, in this case the inductive reactance was an instrumental artefact.

For accurate measurement of the cell impedance it is necessary to select a sense resistor of magnitude of the same order as the test cell. Since the lowest sense resistor incorporated in the

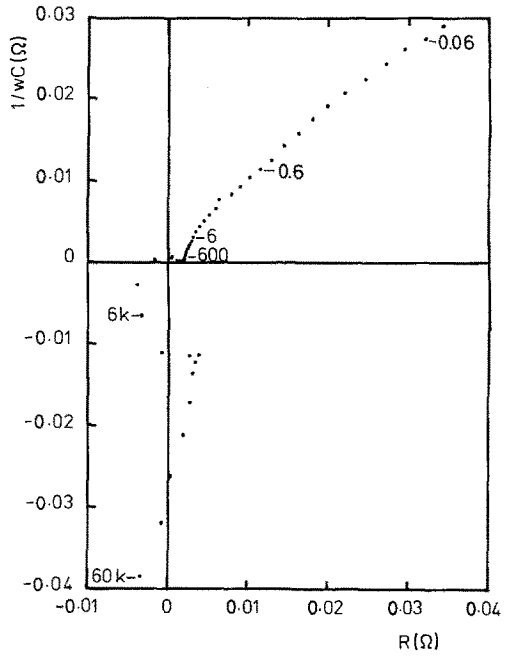

Fig. 1. Impedance spectrum of 25 Ah sealed lead–acid cell using a sense resistor of 10 Ω.

Solartron electrochemical interface is 10 Ω, it is necessary to use an external low-valued resistance of around 0.1 Ω for the impedance measurements of the batteries under investigation.

In order to check the inaccuracies arising due to the differences in the order of magnitude of the sense resistance and the test system, the impedance of a non-inductive grade 1 Ω resistor was measured over the frequency range 60–0.3 kHz using sense resistors of 10 and 100 Ω. The observed impedance spectra were consequently found to be totally different, indicating the importance of the selection of the sense resistor. When an external 1 Ω resistance was used as the sense resistance, the measured resistance values were lower than the expected 1 Ω by around 13% and indicated that for the measured resistance values to be as expected, a sense resistor value of 1.124 Ω has to be used instead of the actual 1 Ω. This additional 0.124 Ω was considered to be arising from the impedance of the electronic path within the 1186 interface which leads up to the socket to which the external sense resistor is connected. Furthermore the measured impedance of the resistance under test varies rapidly at higher frequencies (> 300 Hz) indicating that the effec-

tive impedance of the sense resistor is frequency dependent, probably due to an inductive component. Hence it was found necessary to calibrate the impedance of the sense resistor. Since the internal design of the electrochemical interface introduces a resistance of 0.124 Ω to the external sense resistor, it was decided to calibrate the interface using only a shorting bar as the sense resistor, effectively introducing a resistance of 0.124 Ω as the sense resistor.

2.3. *Calibration procedure*

The impedance of a Tinsley 22 Amp standard resistor (Type 1682) of 0.1 Ω was measured with an accuracy of ± 1% using an Owen bridge assembled with high precision air capacitors and non-inductive metal oxide resistors. All components of the bridge were calibrated with an accuracy of ± 1% prior to the bridge assembly.

The actual layout and the wiring of the bridge was carefully designed in order to avoid unaccounted for residual resistors due to small lengths of wires at the corners of the bridge. The magnitudes of the bridge arms were selected such that the errors due to the stray capacitors were negligible.

The measured values of the resistance (R) and the inductive reactance ($L\omega$) of the standard resistor plotted against frequency (F) are shown in Figs. 2 and 3. The plot of $L\omega$ vs F (Fig. 3) is linear with a correlation coefficient of 0.999, a slope of $1.356 \pm 0.014 \times 10^{-6}$ Ω S and an intercept of $6.08 \pm 1.07 \times 10^{-4}$ Ω.

The plot of R vs F (Fig. 2) is curved; however, a plot of log $(R - 0.100)$ vs log (F) was found to be linear above 4 kHz. The best correlation coefficient 0.999 was obtained for the log plot of $(R - 0.09997)$ as shown in Fig. 4, with a slope of 1.121 ± 0.061 and an intercept of -7.679 ± 0.075. From these relationships for R, $L\omega$ and

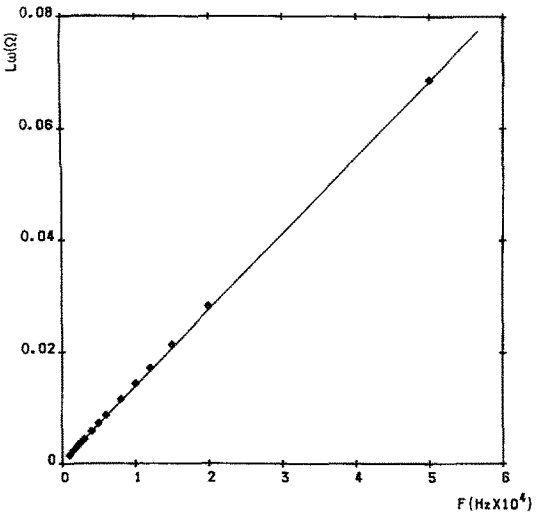

Fig. 3. Variation of the reactance of standard 0.1 Ω resistor with frequency.

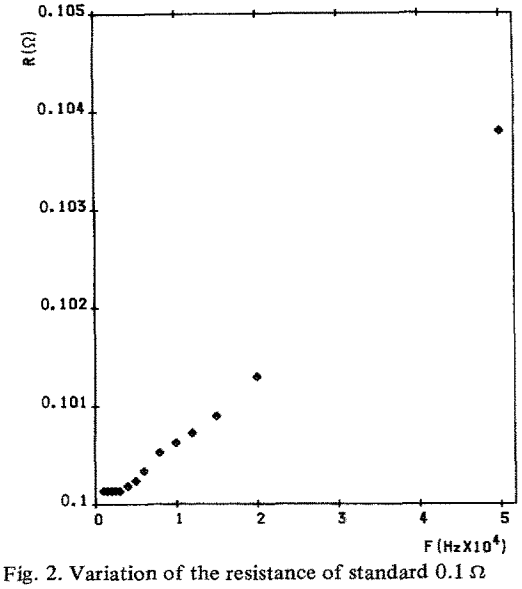

Fig. 2. Variation of the resistance of standard 0.1 Ω resistor with frequency.

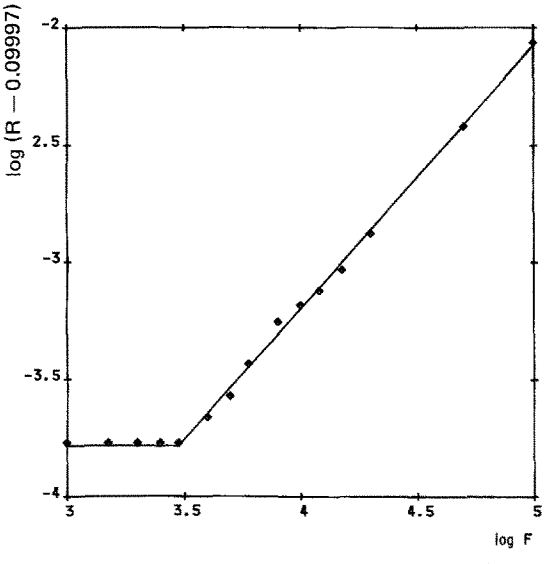

Fig. 4. Linearized plot of the resistance of standard 0.1 Ω resistor.

F the resistance and the inductance of the standard resistor at any specific frequency can be calculated.

The impedance of the standard resistor was measured with the electrochemical interface using a shorting bar as the sense resistor assuming a nominal resistance value of 0.124 Ω only. The measured values of R and $L\omega$ were scattered over a range of 0.001 Ω and the averaged results of 10 replicate measurements are shown against F in Figs. 5 and 6. Using this data and the relationships obtained for R and $L\omega$ from the bridge measurements the nominal value of the sense resistor was corrected to obtain a new set of values for the resistance and the inductance.

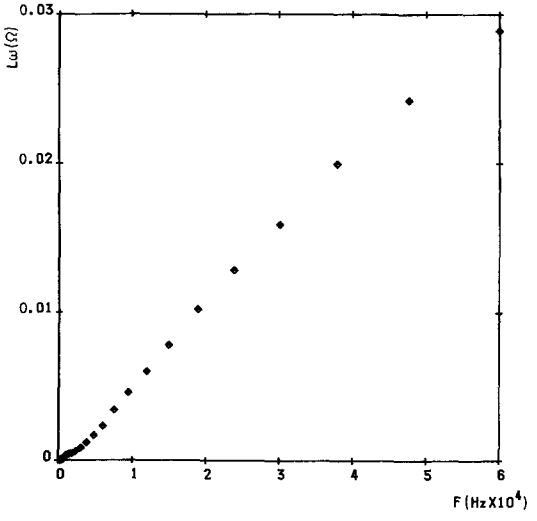

Fig. 6. Inductive reactance corresponding to the experimental data of Fig. 5.

3. Discussion

If Z_s is the effective impedance of the sense resistor including the impedance of the electronic path within the 1186 interface

$$Z_s = S' + jS'' \quad (1)$$

where S' and S'' are the real and imaginary components of the impedance and $j = (-1)^{1/2}$. The actual impedance of the standard resistor is

$$Z_R = R' + jR'' \quad (2)$$

where R' and R'' are the resistance and the reactance of the resistor as obtained from the bridge measurements. Putting the impedance of the standard resistor measured by the Solartron apparatus as

$$Z = X + jY \quad (3)$$

where X and Y are the resistance and reactance of the resistor when a nominal resistance of S is used as the impedance of the sense resistor, then

$$R' + jR'' = \frac{(X + jY)}{S}(S' + jS'') \quad (4)$$

$$(S' + jS'') = \frac{S(R' + jR'')}{(X + jY)} \quad (5)$$

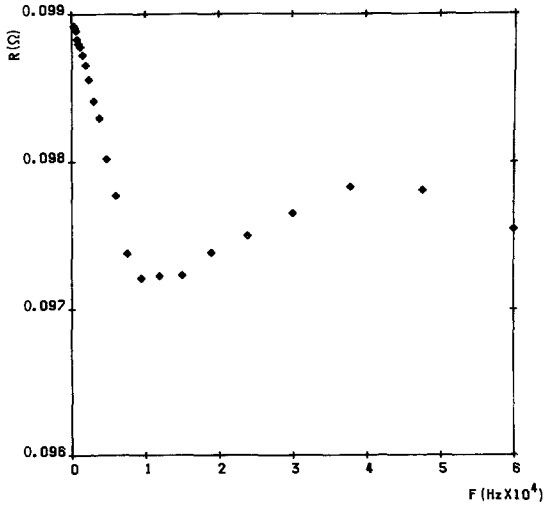

Fig. 5. Plot of resistance vs frequency for the 0.1 Ω standard resistor as measured by the FRA using a nominal value of 0.124 Ω for the sense resistor.

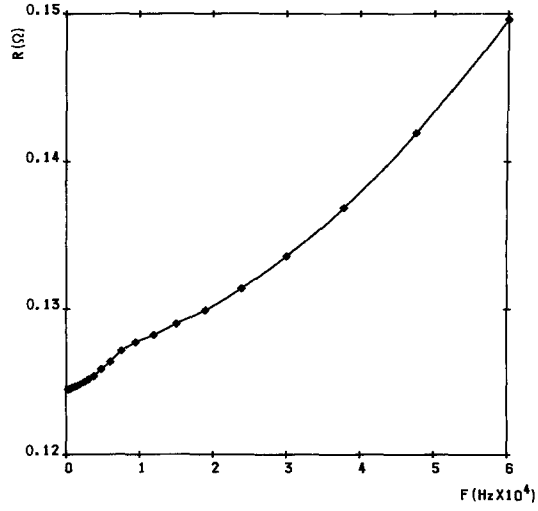

Fig. 7. Calibration curve for the resistance of the sense resistor.

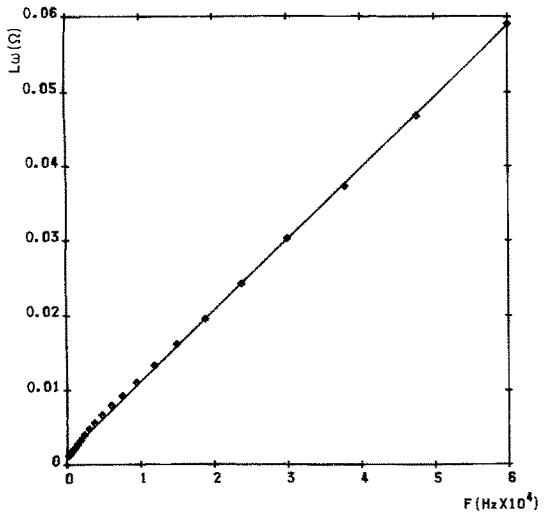

Fig. 8. Inductive reactance corresponding to the experimental data of Fig. 7.

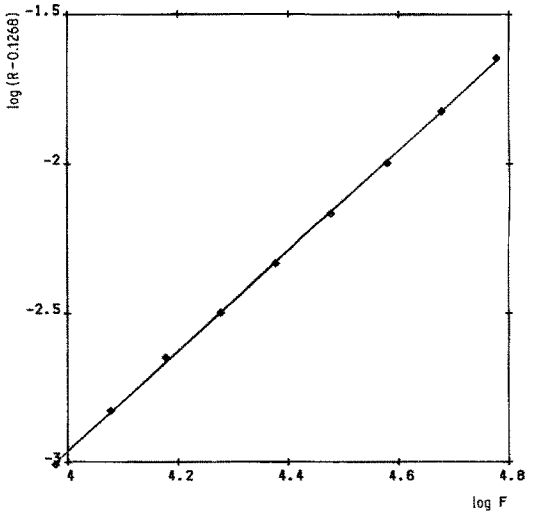

Fig. 10. As Fig. 9, for data in the range 60–9.5 kHz.

and

$$S' = \frac{S(XR' + YR'')}{(X^2 + Y^2)} \tag{6}$$

$$S'' = \frac{S(XR'' - YR')}{(X^2 + Y^2)} \tag{7}$$

The above two expressions can be used to calculate the actual resistance and the reactance of the sense resistor.

The values of resistance S' and reactance S'' thus calculated when plotted against F are shown in Figs. 7 and 8. The variation of the reactance with frequency is linear with a correlation coefficient of 0.999, a slope of $9.57 \pm 0.26 \times 10^{-7}$ and an intercept of $1.509 \pm 0.106 \times 10^{-3}$.

$$L\omega = 9.57 \times 10^{-7} F + 1.509 \tag{8}$$

The variation of the resistance is nonlinear with a kink around 9500 Hz. However, a log plot of $R - R_{\min}$ where $R_{\min}$ is the minimum resistance, 0.1245 Ω, against log F tends to be linear as shown in Fig. 9. The line consists of three distinct sectors, marked by the kinks of the plot of R vs F. The correlation coefficient for the line is 0.993 with slope of 1.29 ± 0.16 and intercept of -7.71 ± 0.12.

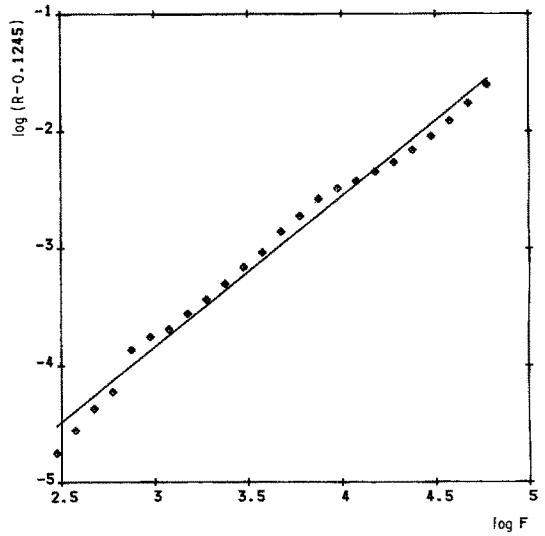

Fig. 9. Approximate 'linear' plot of the data in Fig. 7.

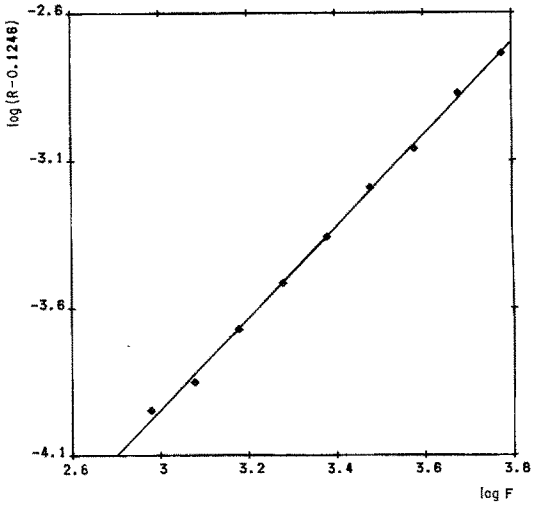

Fig. 11. As Fig. 10, for the range 7.5–0.75 kHz.

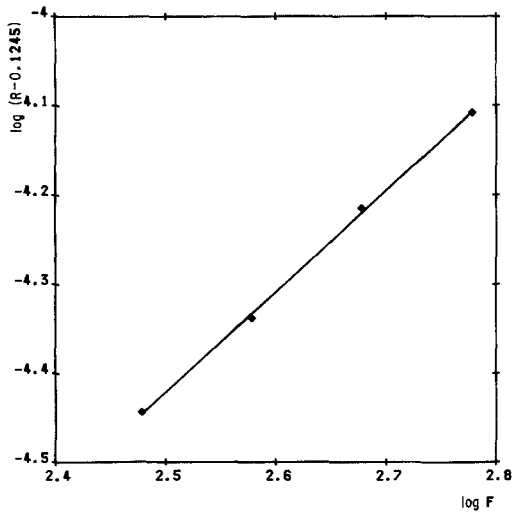

Fig. 12. As Fig. 10, for the range 600–300 Hz.

$$\log (R - 0.1245) = 1.29 \log F - 7.71 \quad (9)$$

More accurate linear plots were obtained by the separation of the data at the kinks, i.e. 60–9.5 kHz, 7.5–0.755 kHz and 600–300 Hz and the selection of three different values of R_{min} for each of the segments. The resulting plots are shown in Figs. 10–12, and the expressions for R and the correlation coefficients are shown below

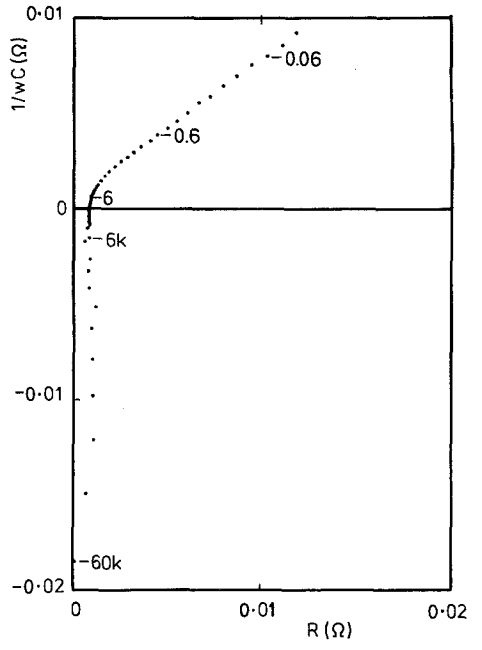

Fig. 13. As Fig. 1, using the calibrated shorting bar as the 'sense impedance'.

At frequencies above 600 Hz the actual resistance can be obtained from Equations 10 and 11, depending on the frequency and the reactance from Equation 8, and these values have to be

60–0.5 kHz	$\log (R - 0.1268) = 1.704 \log F - 9.79$	(cc = 0.999)	(10)
7.5–0.755 kHz	$\log (R - 0.1246) = 1.556 \log F - 8.614$	(cc = 0.999)	(11)
600–300 Hz	$\log (R - 0.1245) = 1.13 \log F - 7.247$	(cc = 0.999)	(12)

In the derivation of Equations 10–12 the values of R_{min} were selected in order to obtain the highest correlation coefficient (cc).

3.1. *Preferred impedance measurement procedure*

When the shorting bar is used, the actual reactance and the resistance of the sense resistor can be obtained from Equations 8 and 10–12, depending on the frequency. At frequencies below 600 Hz the reactance (1.6 mΩ) can be neglected compared to the resistance (124 mΩ) and since the variation of the actual resistance in this region is also negligible, it could be considered as a frequency independent pure resistor of 0.1245 Ω. incorporated in the final calculation of the impedance from the data obtained by the FRA.

For convenience and speedy data acquisition from the FRA a nominal value of 0.1245 Ω for the sense resistance was used during the actual impedance measurements and the data were then corrected for the actual sense resistor impedance, prior to permanent storage of the magnetic disc.

Fig. 13 shows a plot of $(1/\omega C)$ vs R for 25 Ah sealed lead–acid cell obtained according to the above procedure. However, when the impedance data were corrected using the approximate Equation 9 for sense resistance, the resultant plot, Fig. 14, did not show any significant deviation from the more accurately corrected impedance spectra. The slight differences observed

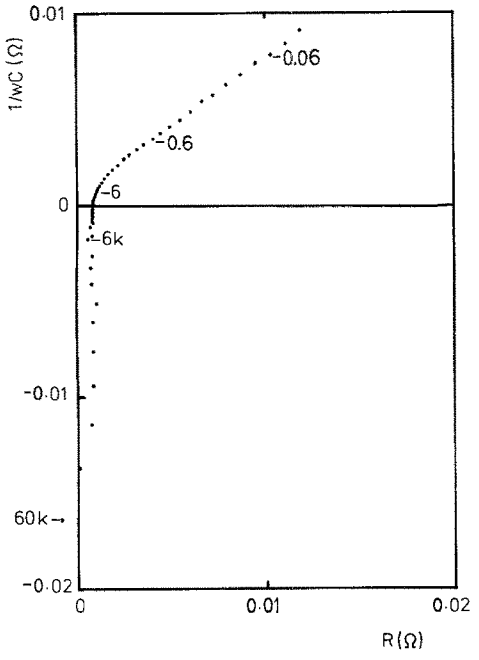

Fig. 14. As Fig. 13, but using a single expression (Equation 9) for the resistance of the 'sense impedance'.

at high frequencies are well within the error limits associated with the FRA data. Hence, for convenience a single expression for the resistance of the sense resistor, Equation 9, can be used instead of the more accurate, but more inconvenient, expressions of Equations 10–12.

4. Conclusions

The errors involved in measuring the impedances of high capacity electrochemical storage cells (especially at high frequency) can be gross. These errors can be eliminated using an appropriate calibration technique.

Acknowledgements

This work has been carried out with the support of the Procurement Executive, Ministry of Defence, UK.

Drs John Knight and Alex Lee are also thanked for their informative discussion.

References

[1] N. A. Hampson and C. Lazarides, *Surf. Technol.* 17 (1982) 205.